Journal of Photochemistry & Photobiology, B: Biology 193 (2019) 1–7

Contents lists available at ScienceDirect

Journal of Photochemistry & Photobiology, B: Biology

journal homepage: www.elsevier.com/locate/jphotobiol

Biosynthesis of silver nanoparticle using extract of *Zea mays* (corn flour) and investigation of its cytotoxicity effect and radical scavenging potential

T. Rajkumar[a], Andras Sapi[a], Gitishree Das[b], Trishna Debnath[c], AbuZar Ansari[d,e,1], Jayanta Kumar Patra[b,*]

[a] Department of Applied and Environmental Chemistry, University of Szeged, H-6720 Szeged, Hungary
[b] Research Institute of Biotechnology & Medical Converged Science, Dongguk University-Seoul, Ilsandong-gu, Gyeonggi-do 10326, Republic of Korea
[c] Department of Food Science and Biotechnology, Dongguk University-Seoul, Ilsandong-gu, Gyeonggi-do 10326, Republic of Korea
[d] Department of Rehabilitation Medicine of Korean Medicine, Dongguk University, Ilsandong-gu, Gyeonggi-do 10326, Republic of Korea
[e] College of Pharmacy, Dongguk University, Ilsandong-gu, Gyeonggi-do 10326, Republic of Korea

ARTICLE INFO

Keywords:
Antioxidant activity
Cytotoxicity activity
Photo-biosynthesis
Photo-catalyzed
Silver nanoparticles
Zea mays

ABSTRACT

Silver nanoparticles (AgNPs) possesses a number of exceptional pharmaceutical properties and applications as compared with other types of metallic nanoparticles. Currently, AgNPs was biosynthesized using an aqueous extract of *Zea mays* L. (corn flour) powder. Further, the effect of concentration of reagents, extract, temperature and time of synthesis was also studied along with the cytotoxicity and radical scavenging potential. UV–vis spectra of AgNPs gave a surface plasmon resonance at ~420 nm. The absorption peak became sharp with the increase in time. AgNPs with monodispersed and aggregated spherical shape was observed by SEM image followed by its confirmation via strong signal in silver region of EDX spectrum. The XRD spectra confirmed its crystallinity and face-centered cubic structure. FT-IR spectra reveal the presence of phytocompounds in the synthesis of AgNPs. Further, the AgNPs exhibited strong cytotoxicity potential against HepG2 cells and its viability declined with an increase in the concentration of AgNP with respect to the control cells. It also demonstrated reasonable radical scavenging potential in terms of DPPH and ABTS scavenging, and reducing power tests. Taken together, these results of the current investigation stated that AgNPs could be beneficial in biomedical applications particularly for treatment of cancer disease along with its applications in pharmaceutical industries for the formulation of new drugs.

1. Introduction

Metal nanoparticles compared to their bulk counterparts possesses a number of physical and chemical properties like catalytic, electrical, optical and magnetic properties [1,2]. In modern years, synthesis of AgNPs drew much attention due to its catalytic [3], optical [4], antibacterial properties [5–7] and substrates for surface-enhanced Raman spectroscopy [8]. Various methods such as physical [9–11], chemical [12–14] and biological approaches [15–18] are being used for the manufacture of silver nanoparticles. The physical method uses highly expensive equipments and also produced large size nanoparticles. While, the chemicals such as sodium borohydride and hydrazine were used as reducing agents in the chemical method of nanoparticle synthesis which are highly hazardous. But, in the case of the biological process, plants and microorganisms were used to synthesize AgNPs. However, microorganisms used in a biological method are sometimes hazardous as they might produce harmful effects. Thus, hazardous chemicals and microorganisms are mostly avoided and plant sources are normally used for the synthesis of AgNPs in a most eco-friendly and cost effective process. Amongst all the biological materials used in the nanoparticle synthesis, the plant extract mediated nanoparticle synthesis is quicker and the synthesized nanoparticles are more stable [19,20]. Moreover, biomolecules present in the plants act as a suitable entity for reduction and stabilization in order to convert Ag^+ to Ag [21,22].

A variety of plants, their parts, and their extracts are being previously utilized in the biological synthesis of a number of metal nanoparticles including silver nanoparticles [23–27]. Recent investigations have revealed that the existence of active functional groups and biological compounds such as sugar, phenolic compounds and flavonoids

* Corresponding author.
E-mail address: jkpatra@dongguk.edu (J.K. Patra).
[1] Present address.

https://doi.org/10.1016/j.jphotobiol.2019.01.008
Received 12 December 2018; Received in revised form 31 December 2018; Accepted 16 January 2019
Available online 17 January 2019
1011-1344/

are mainly responsible for the reduction of metal ions into nanoparticles [28,29]. Maize or corn (*Zea mays* L.) is a cereal belonging to the family Poaceae. It contains carbohydrates, fat, protein, vitamins, and minerals [30]. It has been reported that, most of these biomolecules from the corn are responsible for the formation of AgNPs [31]. Therefore, considering all these facts, in the present study, we attempted AgNPs synthesis by reduction of Ag^+ with the *Zea mays* L. aqueous extract under the photo-catalyzed condition followed by its characterization by UV–Vis spectroscopy, XRD, SEM, EDX, and FT-IR analysis. Further these were also evaluated for their biomedical application in terms of its radical scavenging properties using DPPH, ABTS and reducing power assays along with its cytotoxicity potential against the HepG2 cell line.

2. Materials and Methods

2.1. Materials

Zea mays L. (corn flour) powder was purchased from the local market, Walajabad, Tamilnadu, India. Silver nitrate ($AgNO_3$) is of analytical grade from Qualigens Chemicals, Mumbai, India.

2.2. Preparation of the Zea mays L. (Corn Flour) Extract

10 g of *Zea mays* L. (corn flour) powder was boiled with 100 ml of distilled water in a 500 ml flask at 80 °C in a water bath for 30 min. After cooling, the extracts were filtered using filter paper (Whatman No. 1) and kept in a glass bottle at 4 °C until further analysis.

2.3. Light Mediated Biosynthesis of AgNPs

To bio-synthesize AgNPs, 24 ml of the extract was mixed with 16 ml of 1 mM $AgNO_3$ solution in a 100 ml flask with constant magnetic stirring and exposed to laboratory light for photo-catalyzed condition. A color change of mixture solution from yellow to reddish-brownish coloration indicated the development of colloidal AgNPs with respect to time. The reaction mixture was further centrifuged at 12,000 rpm followed by drying at 60 °C for 2–3 h and later on powdered and stored for analysis.

2.4. Characterization of the Synthesized AgNP

Biosynthesis of AgNPs was monitored at a regular interval using an UV–Vis spectrophotometer (Shimadzu-2450 UV–vis spectrophotometer) in the range between 200 and 800 nm. Data were collected at regular interval of time and the color change was recorded. The nature of the photo-synthesized AgNPs was determined by a XRD machine (X'Pert MRD; PANalytical, Almelo, The Netherlands; machine setup: 40 mA and 30 kV with Cu Kα radians at 2θ angle) using a standardized protocol [32]. The surface morphological characteristics and the primary configuration of the photo-synthesized AgNPs were carried out by SEM (HITACHI S-3000N; Hitachi, Tokyo, Japan) and EDX instruments attached to the SEM machine by standard procedure. The FT-IR analysis was acquired using an FT-IR spectrophotometer (FT-IR Spectrometer; PerkinElmer, Waltham, MA, USA) [33] at different wavelengths (400 cm^{-1} to 4000 cm^{-1}).

2.5. Biopotential of the Synthesized AgNPs

2.5.1. Cytotoxicity Effect of the Photo-Synthesized AgNPs

The cytotoxicity effect of the synthesized AgNPs was tested in the HepG2 cell line by a regular technique with reference to previous literature [32,34]. The morphology of the AgNPs treated cells and its viability were examined by the trypan blue exclusion assay and spotting them under an inverted microscope [32,34].

2.5.2. Free Radical Scavenging Potential of the Photo-Synthesized AgNPs

The free radical scavenging potential of AgNPs was investigated by the DPPH (1,1-diphenyl-2-picrylhydrazyl) assay, ABTS (2,2′-azino-bis [3-ethylbenzothiazoline-6-sulphonic acid]) assay, and reducing power assays using the standard procedures. The DPPH and ABTS scavenging activity of AgNPs and the standard reference compound, gallic acid (GA), was estimated following the standard method of Patra and Baek [35]. The % scavenging effect was calculated as per Eq. (1).

$$\%\text{scavenging effect} = \frac{C_{abs} - T_{abs}}{C_{abs}} \times 100 \quad (1)$$

where C_{abs} is the absorbance of the control value, and T_{abs} is the absorbance of treatment value.

The reducing power of AgNPs was estimated following a standard procedure of Patra and Beak (2017) [35]. The absorbance of the mixture solution was detailed at 700 nm wavelength and the results are deduced as its absorbance value.

2.6. Statistical Analysis

All the data are presented as the mean value of three readings with standard deviation. One-way ANOVA and Duncan's multiple range test using SPSS version 23.0 (IBM Corp., Armonk, NY, USA) was recorded and the values were presented at $P < .05$.

3. Results and Discussion

3.1. UV–Vis Spectroscopy

The development process of the bio-synthesized AgNPs was assessed by UV–visible spectroscopy. Generally, the Surface plasmon resonance (SPR) value is considered for detecting the quality of the synthesized AgNPs [36] and in this study, the SPR band was observed around 410–420 nm for AgNPs which is well within the recommended range for AgNP. SPR peak's position and shape depend on the particle size and shape of the AgNPs [37]. Thus, the observed absorption spectra in this study indicated the presence of small sized, monodispersed AgNPs. According to Mie theory, the presence of single peak around 420 nm corresponds to spherical shaped AgNPs [38] which is also seen in the current study.

3.2. Effect of Different Parameters on the Synthesis of AgNPs

Fig. 1A showed the UV–Vis spectra of AgNPs prepared using 24 ml extract with 16 ml (1 mM) $AgNO_3$ at 100 °C for different time duration. The UV-Vis spectral absorbance maxima gradually sharpened with the increasing time (Fig. 1A). At lower reaction time the SPR band is broad, that indicates broad particle size distribution. More amount of AgNPs was initiated with every increase of time as indicated by the intensity of the SPR band which increases with increasing reaction time. However, at 6 h, the decrease in absorption intensity with broad SPR band indicates the aggregation and broad particle size distribution of AgNPs [39].

The UV–Vis spectral image of the bio-synthesized AgNPs prepared by taking 24 ml of plant extract at 100 °C for 2 h with different $AgNO_3$ concentration (16 ml) is shown in Fig. 1B. For 0.5 mM $AgNO_3$ concentration, ultraviolet-visible spectra showed absorption peak maxima at 417 nm with peak broadening that indicates the synthesized AgNPs are polydispersed in nature. Similarly, the 1 mM $AgNO_3$ solution showed a peak at 420 nm. The red shifts of the peak as the $AgNO_3$ concentration increases, indicated the rise in the diameter of the synthesized AgNPs [40]. However, in the case of 2 mM $AgNO_3$ concentration, the AgNPs synthesis is very less and for 3 mM $AgNO_3$ concentration, there is no formation of AgNPs. This indicated that the optimum concentration of $AgNO_3$ is 1 mM for the maximum manufacture of AgNPs. A similar observation was made by Mittal et al. [41].

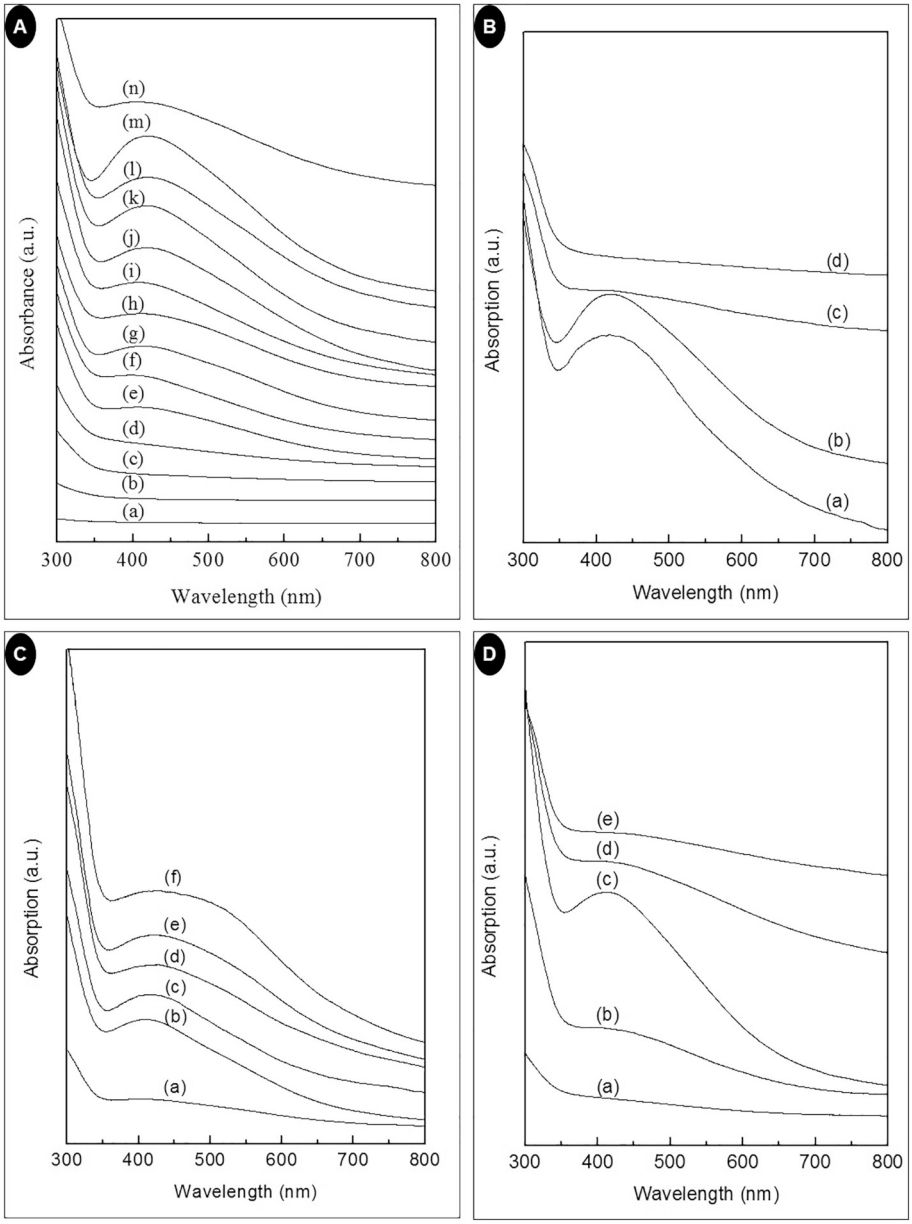

Fig. 1. (A) UV–Vis absorption spectra of AgNPs synthesized at different time interval [(a) $AgNO_3$ (b) *Zea mays* extract (c) 0.5 h (d) 1 h (e) 1.5 h (f) 2 h (g) 2.5 h (h) 3 h (i) 3.5 h (j) 4 h (k) 4.5 h (l) 5 h (m) 5.5 h (n) 6 h]; (B) UV–Vis absorption spectra of AgNPs synthesized at different $AgNO_3$ concentration [(a) 0.5 mM (b) 1 mM (c) 2 mM (d) 3 mM]; (C) UV–Vis absorption spectra of AgNPs synthesized at different extract concentration [(a) 10 ml (b) 20 ml (c) 30 ml (d) 40 ml (e) 50 ml (f) 60 ml]; (D) UV–Vis absorption spectra of AgNPs synthesized at different temperature [(a) 40 °C (b) 60 °C (c) 80 °C (d) 100 °C (e) 120 °C].

Fig. 1C showed the UV–Vis spectral image of the bio-synthesized AgNPs taking different concentrations of the extract and 20 ml of $AgNO_3$ (1 mM) at 100 °C for 4 h. At low extract concentration, Ag^+ was not sufficiently reduced. With increased extract concentration from 10 ml to 30 ml, the absorption band appeared at 418 nm. When the concentration increased further from 30 ml to 60 ml, the absorption intensity progressively increased and the shape of the absorption band become much broader. The results indicated that with increasing concentration of the extract, there is a shrill growth in the quantities of AgNPs with wider size distribution of particles. Similar results were reported in the literature [42].

UV–Vis spectral analysis of AgNPs synthesized using 30 ml extract, 20 ml $AgNO_3$ (1 mM) heated at different temperature for 5.5 h is shown in Fig. 1D. From the results, it was confirmed that increase of the reaction temperature is directly proportional to the manufacture of nanoparticle. The maximum production of AgNPs was observed at 80 °C. This may be due to reduced aggregation of AgNPs at this temperature whereas a further increase in temperature reduced absorption intensity that could be ascribed to the accumulation of crystals around the nucleus of AgNPs already formed [43].

3.3. Characterization of the Bio-Synthesized AgNP

Fig. 2 showed the XRD pattern and nature of the bio-synthesized AgNPs. XRD is an important tool to confirm the crystalline arrangement and nature of the synthesized NPs. The XRD of the prepared AgNPs showed diffraction peaks at 2θ value of 38.2°, 44.42°, 64.4°, 76.7 and 81.45° correspond to (111), (200), (220), (311) and (222) reflections of fcc structure of metallic silver [44]. It indicates that the AgNPs are crystalline in nature AgNPs [45]. The morphological characteristics of the AgNP surface was analyzed by SEM, and the illustrative SEM image magnified at 100 nm and 1000 nm × are shown in Fig. 3A. The SEM

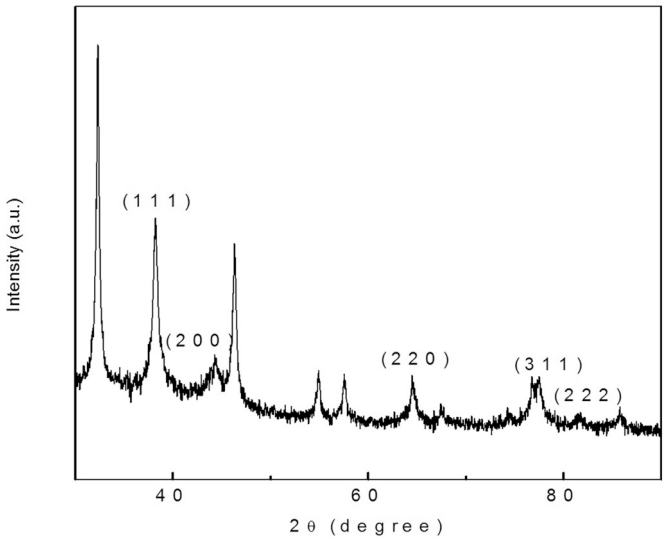

Fig. 2. XRD pattern of AgNPs synthesized using *Zea mays* extract.

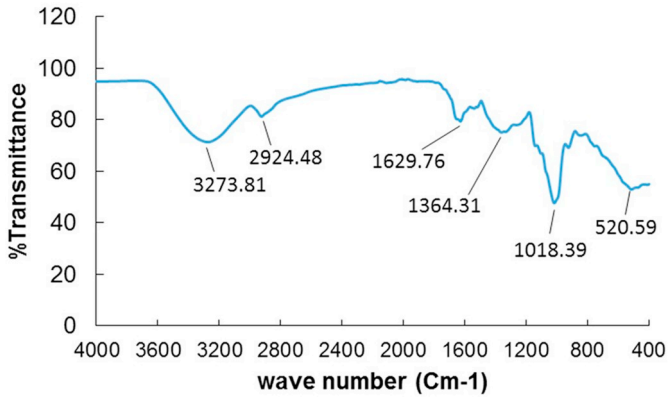

Fig. 4. IR spectra of AgNPs synthesized using *Zea mays* extract.

image clearly reveals the presence of monodispersed and aggregated spherical AgNPs. The EDX results showed strong signal in the silver region with the absorption peak at 3 keV because of the SPR (Fig. 3B). This results corroborates with the earlier published report [46]. The FTIR spectral image of AgNPs synthesized using *Zea mays* extract is shown in Fig. 4. The band observed at 3186 cm^{-1} is due to the O—H

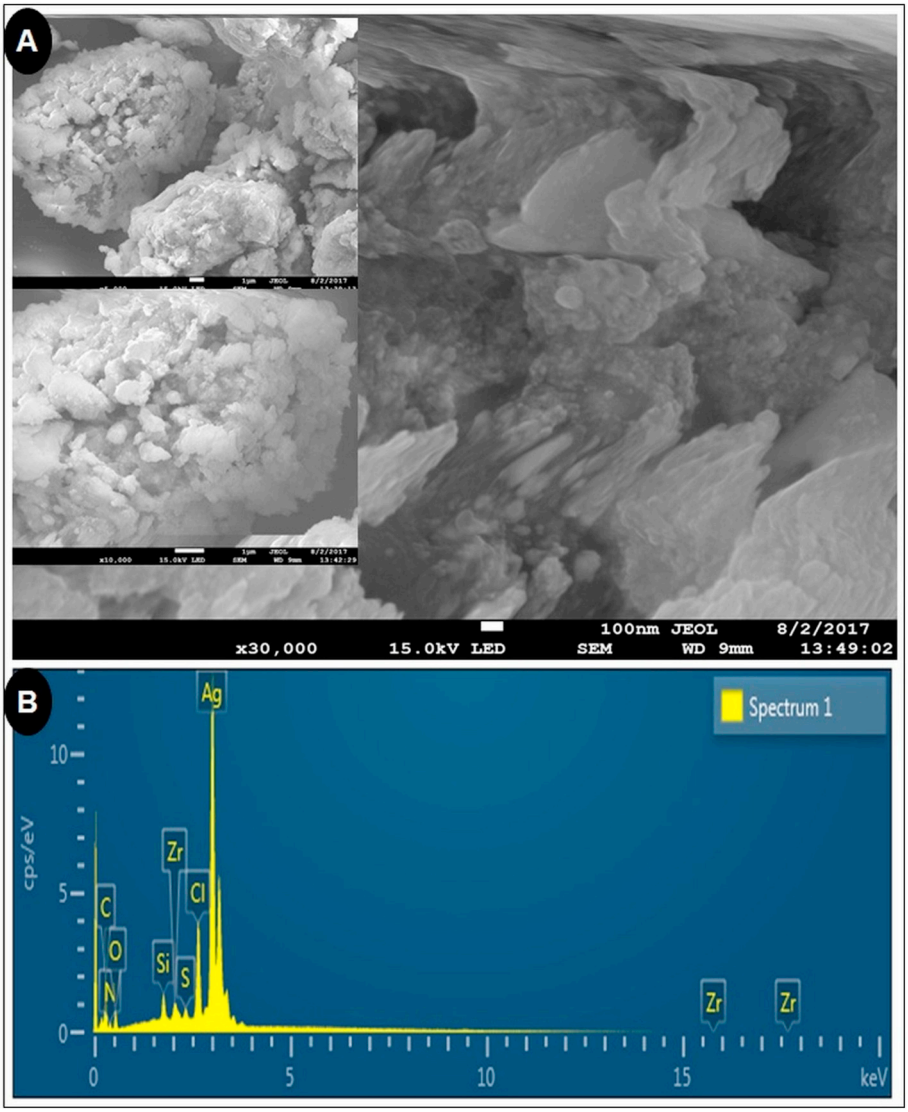

Fig. 3. (A) SEM images and (B) EDX spectra of AgNPs synthesized using *Zea mays* extract.

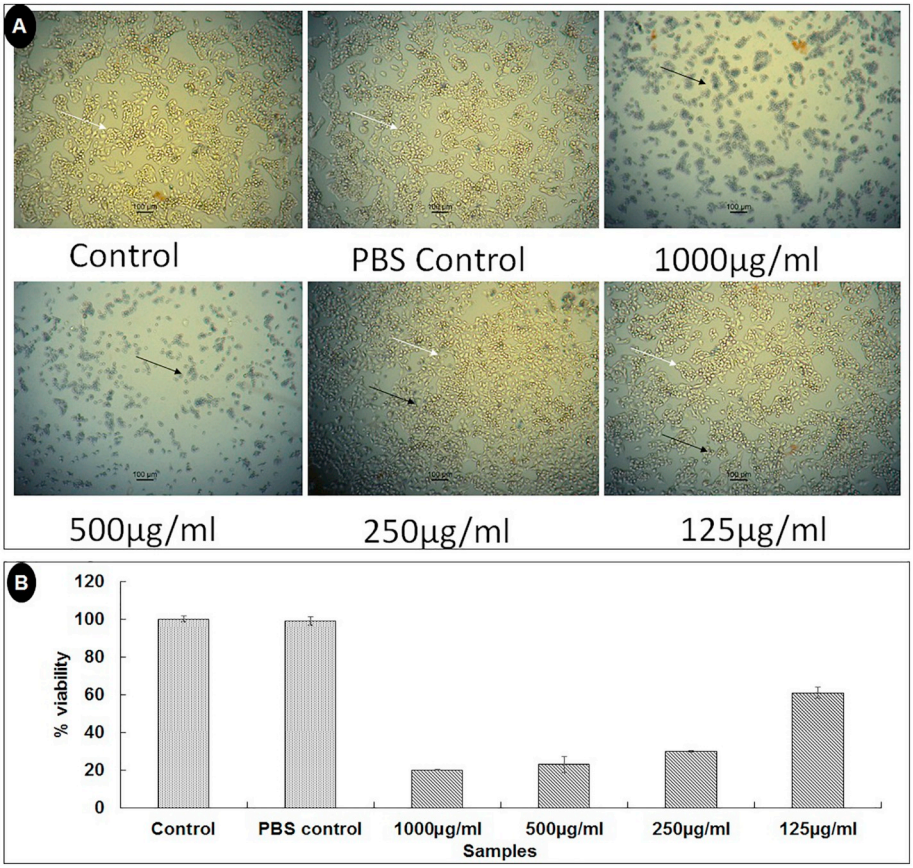

Fig. 5. (A) Cytotoxicity effect of AgNP treatments on HepG2 cell (Black arrow indicating dead cell and white arrow indicating alive cell (× 200 original magnification and 100 µm scale bar)); (B): HepG2 cell viability after treatment of AgNPs for 24 h.

stretching of the phenolic group [47]. The peak at 1726 cm^{-1} is due to carbonyl stretching vibration while the peak at 1651 cm^{-1} can be attributed to C═C stretching vibration. The peak at 1289 cm^{-1} corresponds to the C—O stretching vibration [48]. The peaks at 1545, 1068 cm^{-1} indicates the presence of aromatic and aliphatic amines respectively [49].

3.4. Cytotoxicity and Radical Scavenging Effects of AgNPs

The result of the cytotoxicity potential of the photosynthesized AgNPs against the HepG2 cells of mice is presented in Fig. 5A, B. The Fig. 5A showed the morphological changes such as death of the cell, limited patterns of spreading and increase in the number of cells that floats (black arrows) on the HepG2 cells upon treatment with different concentrations of the treated AgNPs. While in case of the control and low concentration treated images, stable and firmly attached cells were observed (white arrow). In case of Fig. 5B, the cell viability decreased with increased AgNPs concentration. There are a number of hypothesis behind the cytotoxicity potential of the AgNPs [50,51]. Some earlier findings have suggested that the cytotoxicity effect of the AgNPs is basically due to the result of the agglomeration or entry of AgNPs in the nuclei, cytoplasm and other organelles of the treated cells due to smaller particle size and causing damage to the internal organelles of the cells and initiation of different immunological reactions [34,52]. Some researchers have also suggested that the electrostatic attraction between the AgNPs and the cells also could have played a major role in it [19,53]. In the present investigation, the synthesized AgNPs is exhibiting significant cytotoxicity potential which can be related to its anticancer activity and can be further utilized in the anticancer treatment.

The results of the antioxidant potential of the photo-synthesized AgNPs investigated by DPPH scavenging, ABTS scavenging, and the reducing power assays is presented in Fig. 6. The AgNPs and the standard GA (25–100 µg/ml) displayed DPPH scavenging activity that ranged from 84.50% to 97.9% and 85.07% to 96.93% respectively (Fig. 6). While AgNPs (25–100 µg/ml) displayed low ABTS scavenging potential that ranged from 0 to 4.94% as compared to the GA (25–100 µg/ml) taken as the standard compound that ranged from 73.91% to 99.87% respectively (Fig. 6).

Though the AgNPs exhibited high DPPH scavenging activity they showed very less ABTS activity at the same concentrations which might be resulted due to the alteration in the investigational process and steric hindrance between the bioactive compounds from the *Zea mays* extracts those might have taken part in the synthesis process of the tested AgNPs [54]. The AgNPs also displayed less reducing power compared to the standard GA (Fig. 6), which could be due to accumulation of less number of phenolic compounds on the AgNPs surface that are primarily accountable for the reducing action and it also might be a case that other bioactive compounds from the *Zea mays* extracts might have acted as the capping agent on the AgNP surface.

4. Conclusion

Zea mays L. (corn flour) powder aqueous extract was used in AgNPs bio-synthesis that basically acted as the reducing and stabilizing agent. The manufacture of AgNP was illustrated by the SPR peak at 420 nm in the UV–Vis spectra followed by its characterization by SEM, EDX, XRD and FT-IR analysis. The synthesized AgNPs exhibited strong cytotoxicity potential against the HepG2 cells of the mice that increased with the increase in AgNP concentration. It also displayed moderate antioxidant potential. Generally, the results indicated the promising potential of the bio-synthesized AgNPs as a cytotoxicity material that could be useful in the biomedical applications particularly for treatment

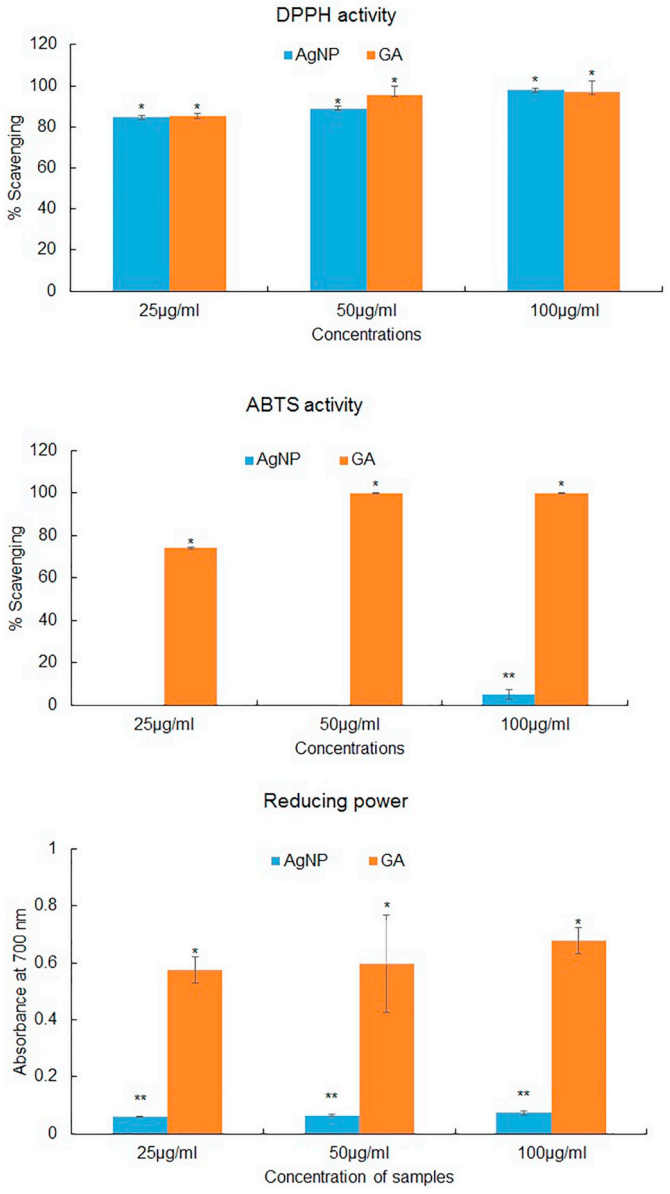

Fig. 6. Radical scavenging potential of AgNPs synthesized using *Zea mays* extract. AgNPs-Silver nanoparticles at different concentration; GA- Gallic acid taken as reference standard. Columns with different superscript symbols are statistically significant at $P < .05$.

against the cancer disease and in the formulation of drugs. Further the *Zea mays* L. (corn flour) powder extract may serve as an effective reducing source of the manufacture of an eco-friendly and cost effective AgNPs for its large scale manufacture and use in pharmaceutical industries.

Acknowledgments

Authors are grateful to Dongguk University, Republic of Korea, for support. Authors are also grateful to Prof. Hojun Kim, Professor, Department of Rehabilitation Medicine of Korean Medicine, Dongguk University, Goyang, Republic of Korea, for providing the laboratory facility for cytotoxicity evaluation.

References

[1] L. Pereira, F. Mehboob, A.J. Stams, M.M. Mota, H.H. Rijnaarts, M.M. Alves, Metallic nanoparticles: microbial synthesis and unique properties for biotechnological applications, bioavailability and biotransformation, Crit. Rev. Biotechnol. 35 (2015) 114–128.
[2] L. Wei, J. Lu, H. Xu, A. Patel, Z.-S. Chen, G. Chen, Silver nanoparticles: synthesis, properties, and therapeutic applications, Drug Discov. Today 20 (2015) 595–601.
[3] K.B.A. Ahmed, R. Senthilnathan, S. Megarajan, V. Anbazhagan, Sunlight mediated synthesis of silver nanoparticles using redox phytoprotein and their application in catalysis and colorimetric mercury sensing, J. Photochem. Photobiol. B Biol. 151 (2015) 39–45.
[4] S.K. Sardana, V.S.N. Chava, V.K. Komarala, Morphology and optical properties of sputter deposited silver nanoparticles on plain, textured and antireflection layer coated textured silicon, Appl. Surf. Sci. 347 (2015) 651–656.
[5] G. Bagherzade, M.M. Tavakoli, M.H. Namaei, Green synthesis of silver nanoparticles using aqueous extract of saffron (Crocus sativus L.) wastages and its antibacterial activity against six bacteria, Asian Pac. J. Trop. Biomed. 7 (2017) 227–233.
[6] D.T. Thuc, T.Q. Huy, L.H. Hoang, B.C. Tien, P. Van Chung, N.T. Thuy, A.-T. Le, Green synthesis of colloidal silver nanoparticles through electrochemical method and their antibacterial activity, Mater. Lett. 181 (2016) 173–177.
[7] Z. Salari, F. Danafar, S. Dabaghi, S.A. Ataei, Sustainable synthesis of silver nanoparticles using macroalgae Spirogyra varians and analysis of their antibacterial activity, J. Saudi Chem. Soc. 20 (2016) 459–464.
[8] E. de Barros Santos, N.V. Madalossi, F.A. Sigoli, I.O. Mazali, Silver nanoparticles: green synthesis, self-assembled nanostructures and their application as SERS substrates, New J. Chem. 39 (2015) 2839–2846.
[9] J.-P. Abid, A. Wark, P.-F. Brevet, H. Girault, Preparation of silver nanoparticles in solution from a silver salt by laser irradiation, Chem. Commun. (2002) 792–793.
[10] S. Kassavetis, S. Kaziannis, N. Pliatsikas, A. Avgeropoulos, A. Karantzalis, C. Kosmidis, E. Lidorikis, P. Patsalas, Formation of plasmonic colloidal silver for flexible and printed electronics using laser ablation, Appl. Surf. Sci. 336 (2015) 262–266.
[11] M. Darroudi, M.B. Ahmad, R. Zamiri, A.H. Abdullah, N.A. Ibrahim, K. Shameli, M.S. Husin, Preparation and characterization of gelatin mediated silver nanoparticles by laser ablation, J. Alloys Compd. 509 (2011) 1301–1304.
[12] Z. Khan, S.A. Al-Thabaiti, A.Y. Obaid, A. Al-Youbi, Preparation and characterization of silver nanoparticles by chemical reduction method, Colloids Surf. B: Biointerfaces 82 (2011) 513–517.
[13] K. Do Kim, D.N. Han, H.T. Kim, Optimization of experimental conditions based on the Taguchi robust design for the formation of nano-sized silver particles by chemical reduction method, Chem. Eng. J. 104 (2004) 55–61.
[14] L. Wang, J. Zhong, G. Li, J.-F. Chen, Preparation of silver nanopowders by a controlled wet-chemical synthesis, Mater. Lett. 173 (2016) 39–42.
[15] J. Du, T.-H. Yi, Biosynthesis of silver nanoparticles by Variovorax guangxiensis THG-SQL3 and their antimicrobial potential, Mater. Lett. 178 (2016) 75–78.
[16] C.S. Espenti, K.K. Rao, K.M. Rao, Bio-synthesis and characterization of silver nanoparticles using Terminalia chebula leaf extract and evaluation of its antimicrobial potential, Mater. Lett. 174 (2016) 129–133.
[17] G.R. Sánchez, C.L. Castilla, N.B. Gómez, A. García, R. Marcos, E.R. Carmona, Leaf extract from the endemic plant Peumus boldus as an effective bioproduct for the green synthesis of silver nanoparticles, Mater. Lett. 183 (2016) 255–260.
[18] Y. San Chan, M.M. Don, Biosynthesis and structural characterization of Ag nanoparticles from white rot fungi, Mater. Sci. Eng. C 33 (2013) 282–288.
[19] P. PS, T. KS, Antioxidant, antibacterial and cytotoxic potential of silver nanoparticles synthesized using terpenes rich extract of Lantana camara L. leaves, Biochem. Biophys. Rep. 10 (2017) 76–81.
[20] S. Iravani, Green synthesis of metal nanoparticles using plants, Green Chem. 13 (2011) 2638–2650.
[21] P.R. Sre, M. Reka, R. Poovazhagi, M.A. Kumar, K. Murugesan, Antibacterial and cytotoxic effect of biologically synthesized silver nanoparticles using aqueous root extract of Erythrina indica lam, Spectrochim. Acta A Mol. Biomol. Spectrosc. 135 (2015) 1137–1144.
[22] K. Kavitha, S. Baker, D. Rakshith, H. Kavitha, H.Y. Rao, B. Harini, S. Satish, Plants as green source towards synthesis of nanoparticles, Int. Res. J. Biol. Sci. 2 (2013) 66–76.
[23] A. Saravanakumar, M. Ganesh, J. Jayaprakash, H.T. Jang, Biosynthesis of silver nanoparticles using Cassia tora leaf extract and its antioxidant and antibacterial activities, J. Ind. Eng. Chem. 28 (2015) 277–281.
[24] S. Joseph, B. Mathew, Microwave-assisted green synthesis of silver nanoparticles and the study on catalytic activity in the degradation of dyes, J. Mol. Liq. 204 (2015) 184–191.
[25] G. Nazeruddin, N. Prasad, S. Waghmare, K. Garadkar, I. Mulla, Extracellular biosynthesis of silver nanoparticle using Azadirachta indica leaf extract and its antimicrobial activity, J. Alloys Compd. 583 (2014) 272–277.
[26] G. Singhal, R. Bhavesh, K. Kasariya, A.R. Sharma, R.P. Singh, Biosynthesis of silver nanoparticles using Ocimum sanctum (Tulsi) leaf extract and screening its antimicrobial activity, J. Nanopart. Res. 13 (2011) 2981–2988.
[27] M. Thirunavoukkarasu, U. Balaji, S. Behera, P. Panda, B. Mishra, Biosynthesis of silver nanoparticle from leaf extract of Desmodium gangeticum (L.) DC. and its biomedical potential, Spectrochim. Acta A Mol. Biomol. Spectrosc. 116 (2013) 424–427.
[28] K. Paulkumar, G. Gnanajobitha, M. Vanaja, M. Pavunraj, G. Annadurai, Green synthesis of silver nanoparticle and silver based chitosan bionanocomposite using stem extract of Saccharum officinarum and assessment of its antibacterial activity, Adv. Nat. Sci. Nanosci. Nanotechnol. 8 (2017) 035019.
[29] H. Zulfiqar, Z. Ayesha, N. Rasheed, Z. Ali, K. Mehmood, A. Mazher, M. Hasan, N. Mahmood, Synthesis of silver nanoparticles using Fagonia Cretica and their antimicrobial activities, Nanoscale Adv. (2019), https://doi.org/10.1039/

C8NA00343B (accepted manuscript).
[30] J.S. Valli, B. Vaseeharan, Biosynthesis of silver nanoparticles by Cissus quadrangularis extracts, Mater. Lett. 82 (2012) 171–173.
[31] A. García-Pérez, M. Harrison, B. Grant, C. Chivers, Microbial analysis and chemical composition of maize (Zea mays, L.) growing on a recirculating vertical flow constructed wetland treating sewage on-site, Biosyst. Eng. 114 (2013) 351–356.
[32] J.K. Patra, G. Das, A. Kumar, A. Ansari, H. Kim, H.-S. Shin, Photo-mediated biosynthesis of silver nanoparticles using the non-edible accrescent fruiting calyx of Physalis peruviana L. Fruits and Investigation of its radical scavenging potential and cytotoxicity activities, J. Photochem. Photobiol. B Biol. 188 (2018) 116–125.
[33] N. Basavegowda, K. Mishra, R.S. Thombal, K. Kaliraj, Y.R. Lee, Sonochemical green synthesis of Yttrium Oxide (Y2O3) nanoparticles as a novel heterogeneous catalyst for the construction of biologically interesting 1, 3-Thiazolidin-4-ones, Catal. Lett. 147 (2017) 2630–2639.
[34] F. Faedmaleki, F.H. Shirazi, A.-A. Salarian, H.A. Ashtiani, H. Rastegar, Toxicity effect of silver nanoparticles on mice liver primary cell culture and HepG2 cell line, Iran. J. Pharm. Res. 13 (2014) 235.
[35] J.K. Patra, K.-H. Baek, Antibacterial activity and synergistic antibacterial potential of biosynthesized silver nanoparticles against foodborne pathogenic bacteria along with its anticandidal and antioxidant effects, Front. Microbiol. 8 (2017) 167.
[36] M. Bindhu, M. Umadevi, Synthesis of monodispersed silver nanoparticles using Hibiscus cannabinus leaf extract and its antimicrobial activity, Spectrochim. Acta A Mol. Biomol. Spectrosc. 101 (2013) 184–190.
[37] K.L. Kelly, E. Coronado, L.L. Zhao, G.C. Schatz, The Optical Properties of Metal Nanoparticles: The Influence Of Size, Shape, and Dielectric Environment, ACS Publications, 2003.
[38] T. Prathna, N. Chandrasekaran, A.M. Raichur, A. Mukherjee, Biomimetic synthesis of silver nanoparticles by Citrus Limon (lemon) aqueous extract and theoretical prediction of particle size, Colloids Surf. B: Biointerfaces 82 (2011) 152–159.
[39] A. Mishra, N.K. Kaushik, M. Sardar, D. Sahal, Evaluation of antiplasmodial activity of green synthesized silver nanoparticles, Colloids Surf. B: Biointerfaces 111 (2013) 713–718.
[40] C. Sudhakar, K. Selvam, M. Govarthanan, B. Senthilkumar, A. Sengottaiyan, M. Stalin, T. Selvankumar, Acorus calamus rhizome extract mediated biosynthesis of silver nanoparticles and their bactericidal activity against human pathogens, J. Genet. Eng. Biotechnol. 13 (2015) 93–99.
[41] A.K. Mittal, D. Tripathy, A. Choudhary, P.K. Aili, A. Chatterjee, I.P. Singh, U.C. Banerjee, Bio-synthesis of silver nanoparticles using Potentilla fulgens Wall. ex Hook. and its therapeutic evaluation as anticancer and antimicrobial agent, Mater. Sci. Eng. C 53 (2015) 120–127.
[42] S. Ahmed, M. Ahmad, B.L. Swami, S. Ikram, Green synthesis of silver nanoparticles using Azadirachta indica aqueous leaf extract, J. Radiat. Res. Appl. Sci. 9 (2016) 1–7.
[43] S. Kaviya, J. Santhanalakshmi, B. Viswanathan, Green synthesis of silver nanoparticles using Polyalthia longifolia leaf extract along with D-sorbitol: study of antibacterial activity, J. Nanotechnol. 2011 (2011).
[44] J. Kasthuri, S. Veerapandian, N. Rajendiran, Biological synthesis of silver and gold nanoparticles using apiin as reducing agent, Colloids Surf. B: Biointerfaces 68 (2009) 55–60.
[45] A. Hebeish, M. El-Rafie, M. El-Sheikh, M.E. El-Naggar, Nanostructural features of silver nanoparticles powder synthesized through concurrent formation of the nanosized particles of both starch and silver, J. Nanotechnol. 2013 (2013).
[46] P.V. Kumar, S. Pammi, P. Kollu, K. Satyanarayana, U. Shameem, Green synthesis and characterization of silver nanoparticles using Boerhaavia diffusa plant extract and their anti bacterial activity, Ind. Crop. Prod. 52 (2014) 562–566.
[47] I. Poljansek, M. Krajnc, Characterization of phenol-formaldehyde prepolymer resins by in line FT-IR spectroscopy, Acta Chim. Slov. 52 (2005) 238.
[48] B. Moldovan, L. David, A. Vulcu, L. Olenic, M. Perde-Schrepler, E. Fischer-Fodor, I. Baldea, S. Clichici, G.A. Filip, In vitro and in vivo anti-inflammatory properties of green synthesized silver nanoparticles using Viburnum opulus L. fruits extract, Mater. Sci. Eng. C 79 (2017) 720–727.
[49] G. Arya, N. Sharma, J. Ahmed, N. Gupta, A. Kumar, R. Chandra, S. Nimesh, Degradation of anthropogenic pollutant and organic dyes by biosynthesized silver nano-catalyst from Cicer arietinum leaves, J. Photochem. Photobiol. B Biol. 174 (2017) 90–96.
[50] S. Ahmed, M. Ahmad, B.L. Swami, S. Ikram, A review on plants extract mediated synthesis of silver nanoparticles for antimicrobial applications: a green expertise, J. Adv. Res. 7 (2016) 17–28.
[51] V.K. Sharma, R.A. Yngard, Y. Lin, Silver nanoparticles: green synthesis and their antimicrobial activities, Adv. Colloid Interf. Sci. 145 (2009) 83–96.
[52] D. He, M.W. Bligh, T.D. Waite, Effects of aggregate structure on the dissolution kinetics of citrate-stabilized silver nanoparticles, Environ. Sci. Technol. 47 (2013) 9148–9156.
[53] Y. Cao, R. Jin, C.A. Mirkin, DNA-modified core − shell Ag/Au nanoparticles, J. Am. Chem. Soc. 123 (2001) 7961–7962.
[54] A.A. Adedapo, F.O. Jimoh, A.J. Afolayan, P.J. Masika, Antioxidant activities and phenolic contents of the methanol extracts of the stems of Acokanthera oppositifolia and Adenia gummifera, BMC Complement. Altern. Med. 8 (2008) 54.